3 4/f

62 70083 527

UNC[redacted]TE

Copy

MEMO 12-11-58E

[redacted]

Change of Security Marking [redacted] 2/15

NASA MEMO 12-11-58E

N63-13887
code-1

553977
38p

NASA

MEMORANDUM

EVALUATION OF INJECTOR PRINCIPLES IN A 2400-POUND-

THRUST ROCKET ENGINE USING LIQUID OXYGEN

AND LIQUID AMMONIA

By Robert C. Hendricks, Robert C. Ehlers,
and Robert W. Graham

Lewis Research Center
Cleveland, Ohio

[redacted]

[redacted]

NATIONAL AERONAUTICS AND
SPACE ADMINISTRATION

WASHINGTON

January 1959

[redacted]

UNCLASSIFIED

[redacted]

NATIONAL AERONAUTICS AND SPACE ADMINISTRATION

MEMORANDUM 12-11-58E

EVALUATION OF INJECTOR PRINCIPLES IN A 2400-POUND-THRUST ROCKET ENGINE USING LIQUID OXYGEN AND LIQUID AMMONIA*

By Robert C. Hendricks, Robert C. Ehlers, and
Robert W. Graham

SUMMARY

The performances of three injector types were evaluated in a 2400-pound-thrust rocket test chamber to compare the relative effects of fuel and oxidant atomization. Injector 1 atomized the fuel and oxidant to a fine degree. Injector 2 atomized the fuel to a coarse degree with straight streams of oxidant. Injector 3 gave coarse oxidant atomization with straight streams of fuel. Each injector represents one of eighteen such units forming the injector for a 50,000-pound-thrust rocket engine.

Characteristic velocity and specific impulse data were obtained over a wide range of oxidant-to-fuel weight ratios at nominal chamber pressures of 600 and 360 pounds per square inch absolute. The performance of injectors atomizing the fuel (injectors 1 and 2) was superior to that of the injector atomizing the oxidant (injector 3), and injector 1, which highly atomized the fuel, gave the highest performance. The throttled performances of injectors 1 and 3 were comparable with their respective high-pressure performances; however, the throttled performance of injector 2 was lower than its high-pressure performance. The performance increase, through atomization, appears to be consistant with the droplet vaporization theory.

Low-frequency instability at the lower chamber pressure was encountered with injector 2 at oxidant-to-fuel weight ratios under 1.3. Combustion instability was encountered spasmodically above this ratio.

The performance data obtained in a 1000-pound-thrust ammonia-oxygen engine with various characteristic combustor lengths are presented to show the effect of increased combustion length and to lend support to the droplet-vaporization theory.

Injector design recommendations necessitate an injector that atomizes the fuel and probably the oxidant.

---

*Title, Unclassified.

[redacted]

INTRODUCTION

Several types of injector elements (spuds) suitable for use with the liquid-ammonia - liquid-oxygen propellant combination were investigated at the NACA Lewis laboratory. These injector elements are similar to those proposed for a 50,000-pound-thrust engine using these propellants. The investigation has been limited to three injector types: the first injector type atomized the fuel and oxidant to a fine degree, the second injector type gave coarse fuel atomization with very coarse oxidant atomization, and the third injector type gave coarse atomization of the oxidant with very coarse fuel atomization. The desire to have an engine throttlable to one-third thrust made it necessary to check injector designs at reduced chamber pressure. Characteristic velocity and specific impulse data, at rated and throttled chamber pressure, determined for each of the injector type from tests of a single spud mounted in a 2400-pound-thrust rocket chamber, are presented. The data of the three injector configurations appear to follow the performance predicted by a model that assumes that the combustion process is controlled by propellant vaporization. Further evidence to support the model predictions is presented in the appendix, where the combustor length was varied to show the effect on performance. The work was completed in unpublished NASA research. Recommendations for injector design requirements are advanced in view of the presented data.

SYMBOLS

A	cross-sectional area, sq in.
C_F	thrust coefficient
c^*	characteristic velocity, ft/sec
c^*_{th}	theoretical characteristic velocity, ft/sec
g	gravitational constant, (lb mass/lb force)(ft/sec^2)
I	specific impulse, (lb force)(sec)/lb mass
$I_{M=1}$	specific impulse at Mach 1
I_{th}	theoretical specific impulse
l	combustor length, in.
l^*	characteristic length, $l^* = l(A_c/A_t)$, in.
O/F	oxidant-to-fuel weight ratio, w_O/w_F

P	pressure, lb/sq in. abs
$\overline{S}$	standard error of estimate
$\overline{S}/c^*_{max}$	characteristic velocity performance-data deviation
$\overline{S}/I_{max}$	specific impulse performance-data deviation
ω	weight flow, lb mass/sec

Subscripts:

a	ambient
c	combustor
e	exit
F	fuel
O	oxidant
t	throat

APPARATUS

Injectors

The three injector configurations evaluated may be seen in figures 1(a) to (c). Injector 1, consisted of 70 pairs of like-on-like impingement fuel holes (0.033 in. diam. nominal) and 66 pairs of like-on-like oxidant holes (0.035 in. diam.) with surface impingement at 56°, with a 60° countersink for discharge purposes. Four showerhead (straight stream) fuel holes and 27 showerhead oxidant holes were added to reduce and equalize the pressure drop. Injector 2 had 22 pairs of like-on-like fuel holes (0.056 in. diam.) with surface impingement at 90° and 22 showerhead oxidant holes (0.061 in. diam., fig. 1(b)). Injector 3 consisted of 22 pairs of like-on-like oxidant holes (0.061 in. diam.) with surface impingement at 90° and 22 showerhead fuel holes (0.053 in. diam., fig. 1(c)). Injector 4, used with a large diameter chamber, consisted of 66 pairs each of like-on-like fuel and oxidant holes with surface impingement at 56° with a 60° countersink for discharge purposes (fig. 1(d)).

The injectors were made of nickel "A". The oxidant injection holes were fed from a plenum chamber on the upstream side of the injector face. The fuel injection holes were fed by passages, cross-drilled through the

[redacted]

injector, from a fuel manifold around the periphery of the injector. Injector 1 had enlarged fuel-feed passages to reduce the very high cross-flow velocities that were characteristic of injectors 2 and 3. Injectors 2 and 3 were designed to deliver 6.1 pounds per second of oxidant and 4.9 pounds per second of fuel at an injector pressure drop of 190 pounds per square inch. Injector 1 was designed to deliver the same flow rate at a pressure drop of 170 pounds per square inch.

Spray tests of injectors 4 and 2 with JP-4 fuel revealed qualitatively the degree to which each injector atomized the fuel. Injector 4 gave "mistlike" atomization while injector 2 gave droplet atomization, which coagulated and formed "solid" streams.

The injector holders were made from stainless steel, designed to provide fuel and oxidant manifolding, and flanges for mounting the engine configuration on the thrust stand (fig. 2).

Chamber and Nozzle

The thrust chamber used consisted of a 5-inch outside diameter mild steel pipe, 6 inches in length, bored to a 3.048-inch inside diameter. The inner wall of the chamber was covered with a 0.012-inch Nichrome base and a 0.010- to 0.015-inch aluminum oxide coating.

The nozzles were made of copper, some having a 0.003- to 0.005-inch chromium plating. Each nozzle had a throat area of 3.26 square inches, a contraction ratio of 2.18, and the diverging section was eliminated. The engine was sealed by eight tension bolts and two metal O-rings. One O-ring was placed between the injector holder and the chamber, and the other between the chamber and the nozzle (fig. 2).

PROCEDURE

A flow diagram of the test facility may be seen in figure 3. The difficulties in igniting the ammonia-oxygen propellant combination were overcome by using a high-voltage coaxial cable, which was inserted into the engine through the nozzle (fig. 2). During ignition, this ignitor was ejected from the engine by combustion gases. Little difficulty was encountered in engine starting. The cable shield was grounded and the copper core was stripped of approximately 2 inches of insulation and bent to form an arc gap between it and the grounded shield. The 10,000-volt, 23-milliampere secondary of a transformer was used to supply a continuous high-energy ignition source. The average run length after steady-state operating conditions were achieved was 1.5 seconds.

[redacted]

Instrumentation

The engine was mounted on a flexure-plate thrust stand equipped with a strain-gage force-measuring load cell. Both oxidant and fuel flow were measured with two instruments, namely, a turbine-type flowmeter and a differential pressure meter equipped with a differential pressure transducer. Chamber-pressure taps were located in the chamber wall near the injector face and near the entrance to the convergent nozzle. These chamber-pressure measurements were sensed by strain-gage transducers. In order to minimize temperature effects on the transducers, 2-foot long, water-cooled, pressure lines to the pickups were used. The temperature of the liquid oxygen was measured by thermocouples in the liquid-oxygen line with the cold-conjunction thermocouples in a bath of liquid nitrogen. The liquid ammonia temperature was recorded by thermocouples in the ammonia line with room temperature thermocouples used as reference. The chamber pressure measured near the injector was recorded on a strip-chart recording potentiometer. The other chamber pressure, temperatures and flow rates of propellants, and thrust were recorded on an oscillograph.

An accelerometer was mounted on the thrust chamber to provide a means to determine whether or not combustion oscillations were occurring. The accelerometer responded to the magnitude and frequency of radial accelerations caused by pressure oscillations within the chamber. The signal from the accelerometer and a 1000-cycle-per-second reference signal were received by a dual-beam oscilloscope and photographed by a high-speed camera.

Calibrations

The pressure transducers were calibrated before each series of runs with helium gas and with standard gages with rated accuracies of ±1/4 percent. The thrust stand, together with the load cell, was also calibrated before each series of runs with a standard load cell with a rated accuracy of ±1/4 percent. Millivolt calibrations of the thermocouples and their recording systems were made intermittently. Fixed-point temperature calibrations were made prior to each run series, using liquid nitrogen and liquid oxygen for the oxygen thermocouples and melting ice and measured room temperature water for the ammonia thermocouples.

Errors in Measuring Performance

Although the individual instruments, the load cell, pressure transducers, flowmeters, strip-chart potentiometer, and recording oscillograph, were rated at ±1 percent or better, several errors present reduced the accuracy of performance measurements. The nonuniformity of the oxygen temperature with time increased the error in determining oxygen mass flow by approximately ±1 percent. The thrust stand and thrust load cell were used at less than one-half capacity thus raising the possible error to ±2.5 percent of rated engine thrust. Hysteresis was observed in combustion-chamber pressure measurement, probably because of a combined effect of the transducer and the strip-chart recorder. The maximum error in measuring c^* and I has been estimated to be 3.0 and 4.5 percent, respectively.

Curvilinear correlation (ref. 1) showed that the experimentally observed deviation in measuring c^* and I, $(\overline{S}/c^*_{max}$ and $\overline{S}/I_{max})$, performance data at rated thrust varied between 0.5 to 1.5 percent and 2.5 to 4.9 percent, respectively. The experimentally observed deviation in measuring c^* and I at throttled thrust varied between 0.4 to 2.1 percent and 0.9 to 2.7 percent, respectively. The experimentally observed deviation in unstable data measurement for c^* and I was 8.2 and 9.2 percent, respectively.

Theoretical c^* (fig. 13) and theoretical I (fig. 14) are based on equilibrium composition because the combustor conditions are closer to equilibrium than frozen.

RESULTS AND DISCUSSION

Injector Performance Evaluation

Injectors 1, 2, and 3 were tested at the rated chamber pressure (600 lb/sq in. abs) with some comparative results shown in the following table:

Injector	Type of atomization	Characteristic velocity, c^* at O/F = 1.25, ft/sec	Specific impulse, I at O/F = 1.25, $\frac{(\text{lb force})(\text{sec})}{\text{lb mass}}$	Maximum performance values				Oxidant-to-fuel weight ratio range	Accelerometer average range, $\frac{\text{cycles}}{\text{sec}}$
				c^*	O/F	I	O/F		
1	F and O, fine impingement	5440	207	5450	1.30	207	1.30	0.65 to 1.30	6000 to 8000
2	F, coarse impingement; O, showerhead	5370	202	5380	1.20	202	1.30	1.05 to 1.40	5000 to 7000
3	O, coarse impingement; F, showerhead	5220	182	5250	1.38	183	1.38	0.85 to 1.40	1500 to 5000

Injector 1, atomizing the fuel and oxidant to a fine degree gave the highest steady-state performance (which is summary plotted in figs. 4(a) and 5(a)). The scatter in performance data was within the predicted experimental error with the exception of the specific impulse of injector 3, which exceeded the limits by 0.5 percent. Injector 2, atomizing the fuel to a lesser degree gave c^* performance data approximately 70 feet per second below that of injector 1 at $O/F = 1.25$. Data from unstabilized runs (dashed line of fig. 6) indicate the values of c^* for an O/F range of 0.75 to 1.5.

Injector 3, which did not atomize the fuel, gave the lowest performance. The increase in performance with increased fuel atomization is substantiated by the results of references 2 and 3. Injectors 1, 2, and 3 showed that the effect of oxidant atomization on performance was of second order; however, atomization of the oxidant seemed to stabilize combustion at other than design thrust for the configuration used. The secondary influence of oxidant atomization on performance is corroborated in reference 4. The performance data of this report, obtained using the small-diameter combustor (see fig. 2), was unmarred by burnouts due to combustion oscillations, for the three injector configurations used.

Some preliminary runs, made with a large diameter chamber (4.072 in.) and injector 4, resulted in chamber burnout from combustion oscillations. The frequency of the oscillations encountered in the large-diameter chamber were up to 12,000 cycles per second. The oscillation amplitudes in the large-diameter chamber were an order of magnitude greater than those encountered with the same injectors in the small-diameter chamber.

Because of the small amplitude, oscillations observed in the small-diameter chamber were considered to have little effect on performance. When the large-diameter chamber was used, the influence of combustion oscillations on performance and their devastating effects were reflected in high c^* and I values and in engine burnout. For example, when injector 4 (fig. 1(d)) was run in a large-diameter chamber resulting in engine burnout, instability raised c^* by 4.8 percent and I by 2.5 percent. Oscillations encountered while running injector 2 were of negligible amplitude in both combustor configurations. The c^* and I performance data obtained at rated chamber pressure are shown in table I, and summarily plotted in figures 4(a) and 5(a). Figures 6 and 7 show the c^* and I performance data, plotted from table I, for injectors 1, 2, and 3.

Engine Throttling

An engine designed to be operated from throttled thrust to rated thrust will have a lower injection pressure drop at throttled thrust than at rated thrust. Combustion instability and poor efficiency may result. A portion of the test program was therefore devoted to throttled performance tests at a chamber pressure of 360 pounds per square inch absolute. The values of c^* should change little with pressure (ref. 5). The c^* and I performance data obtained for throttled chamber pressure are shown in table II and summary plotted in figures 4(b) and 5(b).

Figures 8 and 9 show the c^* and I performance data, plotted from table II, for injectors 1, 2, and 3. The following table gives a comparison of the characteristic velocity at throttled performance with that at rated performance.

Injector	Type of atomization	Characteristic velocity, c^*, ft/sec, at -		Maximum characteristic velocity, c^*, ft/sec, at -			
		O/F = 1.25, P_c = 360 lb/sq in. abs	O/F = 1.25, P_c = 600 lb/sq in. abs	P_c = 360 lb/sq in. abs		P_c = 600 lb/sq in. abs	
				c^*	O/F	c^*	O/F
1	F and O, fine impingement	5380	5440	5385	1.20	5450	1.30
2	F, coarse impingement; O, showerhead	5020	5370	5130	1.55	5380	1.20
3	O, coarse impingement; F, showerhead	5150	5220	5240	1.57	5250	1.38

A comparison of specific impulse at throttled performance with that at rated performance is given in the following table:

Injector	Type of atomization	Specific impulse, I, $\frac{\text{(lb force)(sec)}}{\text{lb mass}}$, at -		Maximum specific impulse, I, $\frac{\text{(lb force)(sec)}}{\text{lb mass}}$, at -			
		O/F = 1.25, P_c = 360 lb/sq in. abs	O/F = 1.25, P_c = 600 lb/sq in. abs	P_c = 360 lb/sq in. abs		P_c = 600 lb/sq in. abs	
				I	O/F	I	O/F
1	F and O, coarse impingement	202	207	202	1.25	207	1.30
2	F, coarse impingement; O, showerhead	161	202	188	1.85	202	1.30
3	O, coarse impingement; F, showerhead	177	182	181	1.49	183	1.38

Injectors 1 and 3 gave throttled performance comparable with rated performance; however, the maximum c^* for injector 3 occurred at a much higher oxidant-to-fuel weight ratio. Injector 1, which highly atomized the propellants, gave stable, efficient performance at low injection pressure drops. Injector 2 gave poor results at the reduced pressure level. It should be noted here for injector 2 that while the c^* values were decreased, the I values remained slightly above the I values found for injector 3 (fig. 5(b)). A hydraulic phenomenon encompassing the oxidant valve, injector, and combustion chamber produced unstable performance data for all c^* values under an O/F of 1.3. A few stable performance points above O/F = 1.3 were obtained; however, instability was spasmodic. The hydraulic phenomenon was not identified as chugging, although strongly suspected, because oxidant valve oscillations were very closely in phase with injection (fuel and oxidant) and chamber-pressure oscillations. It is interesting to note that the other injectors that impinged the oxidant were stable at reduced thrust. The nonatomized oxidant appears to give nonuniformity of oxidant concentration about the fuel droplet. This seems to make an unstable aerodynamic and thermochemical environment, capable of producing pressure oscillations. From these data, it appears that for this particular configuration (injector 2) the instability could be eliminated by oxidant impingement.

The performance level of a rocket engine depends on the combustor geometry as well as the injector design. Combustor length or the parameter l in $l^* = l\,(A_c/A_t)$ has been used to classify the combustor size. In another investigation using a 1000-pound-thrust engine, variation in engine performance with the l parameter was obtained and the results are given in the appendix. These data show that an increase in l results in an increase in performance.

The experimental data presented herein have shown that performance can be improved by an injector which finely atomizes the fuel or by increasing the combustor length. Increasing the combustor length allows more time for all processes to occur, one of which is vaporization.

Similar improvement in performance has been observed with hydrocarbon fuels (ref. 6). Estimates of the degree of performance improvement as a function of the degree of fuel atomization have been made analytically. A theory based on a model which assumes that fuel vaporization controls the combustion process has made possible these analytical estimates. The droplet vaporization theory advanced in references 7 to 10 shows that the burning of liquid fuel droplets depends on the mean initial diameter of the droplets. The theory predicts higher engine performance as the size of the droplet is decreased. The data presented herein seem to follow these general performance predictions. A decrease in the injection-hole diameter results in a decrease of the mean droplet diameter observed in reference 11. Since droplet vaporization is the basis of the theory and considered rate controlling, vaporization appears to be rate controlling for the liquid-ammonia - liquid-oxygen propellant combination.

Injector Design Recommendation

Results indicate that fuel atomization is of primary importance in improving performance of the liquid-ammonia - liquid-oxygen propellant system. The method of fuel atomization is of secondary importance provided that unstable combustion or injector face burning are not results from the atomization method. Oxidant atomization is of secondary importance, although it appears to have some bearing on combustion stability. Thus, an efficient injector will atomize the fuel and from the stability standpoint will probably atomize the oxidant (injector 2).

SUMMARY OF RESULTS

The results found with 2400-pound-thrust-engines using liquid-ammonia and liquid-oxygen propellants are as follows:

1. The finer the degree of fuel atomization, the higher the engine performance; however, comparable performance could possibly be obtained with coarser fuel atomization if a large combustor length is utilized.

2. Oxidant atomization has a secondary effect on engine performance; however, oxidant atomization appeared to stabilize the combustion at other than design thrust for the configuration used.

3. Combustion oscillations can be reduced, and in some cases eliminated, by a change in the combustor configuration.

4. In the liquid-ammonia - liquid-oxygen system, vaporization appears to be rate controlling, as the performance seems to follow that predicted by the droplet vaporization theory.

5. Throttled performance showed injectors that atomized the oxidant to be comparable with their respective values at full thrust. The injector that poorly atomized the oxidant gave unstable performance at reduced thrust.

6. In general, an efficient liquid-ammonia - liquid-oxygen injector at high or low thrust levels will atomize the fuel and probably atomize the oxidant.

Lewis Research Center
National Aeronautics and Space Administration
Cleveland, Ohio, September 18, 1958

APPENDIX - VARIATION IN ENGINE PERFORMANCE WITH l PARAMETER

The performances of other injector and chamber configurations using liquid-ammonia - liquid-oxygen propellants were evaluated at the 1000-pound-thrust level (unpublished NASA data).

The injector evaluated (fig. 10) featured 82 sets of fuel and 70 sets of oxidant like-on-like impingement pairs, subsurface impingement at 90°, and a pressure drop of 70 pounds per square inch. The engine used water-cooled chambers with l parameters of 5.19, 7.78, and 13.0 inches, with the inside diameter held constant at 2.36 inches. The nozzle in all cases had a contraction ratio of 3.85 and expanded to 14.7 pounds per square inch absolute (see fig. 11).

The c^* and I values obtained are shown in figure 12 for l values of 5.19, 7.78, and 13.0 inches. Engine performance in the three chambers improved as the chamber length was increased. This effect is illustrated by the following table which gives c^* values obtained at O/F = 1.25, and the maximum c^* and O/F values (fig. 12) for an injector type that atomized the fuel and oxidant to a fine degree (fig. 10).

l, in.	c^* at 1.25 O/F, ft/sec	Max. c^*, ft/sec	
		c^*	O/F
5.18	5100	5100	1.15
7.78	5220	5220	1.25
13.0	5275	5280	1.22

The presented performance indicates that the necessity for good atomization is reduced as the chamber length is increased. It appears that it is possible to obtain good performance in a large chamber with an injector that gives a low degree of fuel atomization (injector 3 of this report).

REFERENCES

1. Ezekiel, Mordecai: Methods of Correlation Analysis. John Wiley & Sons, Inc., 1956.

2. Canright, Richard B., and Bertrando, B, R.: A Partial Survey of Injector Types, Utilizing the NH_3-O_2 Propellant. Prog. Rep. 1-83, Jet Prop. Lab., C.I.T., June 10, 1952. (Contracts W535-ac-20260, Air Materiel Command; DA-04-495-Ord 18, Dept. Army, Ord. Corps.)

3. Priem, Richard J., and Clark, Bruce J.: Comparison of Injectors with a 200-Pound-Thrust Ammonia-Oxygen Engine. NACA RM E57H01, 1958.

4. Hendricks, Robert C., Ehlers, Robert C., and Humphrey, Jack C.: Evaluation of Three Injectors in a 2400-Pound-Thrust Rocket Engine Using Liquid Oxygen and Liquid Ammonia. NACA RM E58B25, 1958.

5. Gordon, Sanford, and Glueck, Alan R.: Theoretical Performance of Liquid Ammonia with Liquid Oxygen as a Rocket Propellant. NACA RM E58A21, 1958.

6. Heidmann, M. F., and Auble, C. M.: Injection Principles from Combustion Studies in a 200-Pound-Thrust Rocket Engine Using Liquid Oxygen and Heptane. NACA RM E55C22, 1955.

7. El Wakil, M. M., Priem, R. J., Brikowski, H. J., Myers, P. S., and Uyehara, O. A.: Experimental and Calculated Temperature and Mass Histories of Vaporizing Fuel Drops. NACA TN 3490, 1956.

8. Spalding, D. B.: Combustion of Fuel Particles. Fuel, vol. XXX, no. 6, June 1951, pp. 121-130.

9. Spalding, D. B.: Combustion of Liquid Fuel in a Gas Stream, pt. I. Fuel, vol. XXIX, no. 1, Jan. 1950, pp. 2-7; cont., pt. II, vol. XXIX, no. 2, Feb. 1950, pp. 25-32.

10. Agafanova, F. A., Gurevich, M. A., and Paleev, I. I.: Theory of Burning of a Liquid Fuel Drop. Soviet Physics Technical Physics, vol. 2, no. 8, August 1957, (Translation of the Journal of Technical Physics of the USSR, vol. 27, no. 8, published by the American Institute of Physics, May 1958.)

11. Ingebo, Robert D.: Drop-Size Distribution for Impinging-Jet Breakup in Airstreams Simulating the Velocity Conditions in Rocket Combustors. NACA TN 4222, 1958.

[redacted]

TABLE I. - CHARACTERISTIC VELOCITY AND SPECIFIC IMPULSE AT RATED THRUST

Number	Injector	Reference run	Oxidant-to-fuel weight ratio, O/F	Characteristic velocity, c^*, ft/sec	Theoretical characteristic velocity[a], $\frac{c^*}{c^*_{th}}$, percent	Specific impulse[b], I, $\frac{(\text{lb force})(\text{sec})}{\text{lb mass}}$	Theoretical specific impulse[a], $\frac{I}{I_{th}}$, percent
1	1 (see fig. 1(a))	434	0.64	4450	92	180	88
2		436	.88	5290	97	206	96
3		437	1.16	5460	94	210	96
4		438	1.18	5400	93	206	94
5		439	1.30	5500	94	208	96
6		441	.77	4990	96	189	90
7		442	.89	5220	96	196	91
8		443	.74	4980	98	188	90
9		444	1.00	5220	93	195	90
10		445	1.12	5350	93	199	91
11		507	.85	5270	98	202	94
12		508	1.11	5420	94	206	94
13	2 (see fig. 1(b))	419	1.52	4780	84	174	81
14		420	1.35	5270	91	194	89
15		421	1.04	5330	94	196	90
16		422	.65	4500	93	170	83
17		423	.91	4710	86	177	82
18		424	1.37	5320	92	198	91
19		426	1.20	5370	93	204	94
20		458	1.40	5270	91	202	94
21		459	1.28	5350	92	206	94
22		467	1.53	5120	90	196	91
23		468	1.28	5410	93	198	91
24		501	1.26	5290	91	198	91
25		502	1.27	5330	92	200	92
26	3 (see fig. 1(c))	405	1.35	5210	90	189	87
27		406	1.27	5230	90	181	83
28		407	.85	4860	90	167	78
29		408	1.05	5110	90	180	83
30		409	1.22	5360	92	203	93
31		410	1.29	5160	89	183	84
32		411	1.16	5170	90	177	81
33		412	1.01	5010	89	174	80
34		413	1.41	5250	91	181	84

[a]Theoretical values based on equilibrium composition; chamber pressure, P_c, 600 lb/sq in. abs (figs. 13 and 14).

[b]Experimental specific impulse for convergent nozzle expanded to ambient conditions.

[redacted]

TABLE II. - CHARACTERISTIC VELOCITY AND SPECIFIC IMPULSE AT THROTTLED THRUST

Number	Injector	Reference run	Oxidant-to-fuel weight ratio, O/F	Characteristic velocity, c^*, ft/sec	Theoretical characteristic velocity[a], $\frac{c^*}{c^*_{th}}$, percent	Specific impulse[b], I, $\frac{\text{(lb force)(sec)}}{\text{lb mass}}$	Theoretical specific impulse[a], $\frac{I}{I_{th}}$, percent
1	1	446	1.11	5390	94	200	92
2	(see fig.	447	1.02	5250	93	198	91
3	1(a))	448	.64	3920	82	164	80
4		449	1.17	5340	92	202	93
5		503	.83	5160	97	188	88
6		504	1.01	5250	93	198	91
7		505	1.15	5310	92	202	92
8		506	1.39	5300	91	201	93
9		509	1.32	5250	90	197	91
10		511	1.61	5100	90	194	91
11	2	427	1.07	4680	82	176	80
12	(see fig.	428	1.28	4810	83	184	84
13	1(b))	429	1.14	5060	88	192	88
14		450	.57	2870	63	102	52
15		451	1.02	4390	78	176	81
16		452	1.13	4910	85	194	89
17		453	1.00	2760	49	110	50
18		454	.72	4130	82	161	77
19		455	.54	2810	--	112	58
20		456	.59	3360	--	130	69
21		457	.62	3090	65	126	62
22		461	1.28	4990	86	171	78
23		462	1.47	4990	87	176	81
24		463	1.56	5120	90	181	84
25		464	1.62	5180	92	183	86
26		465	1.54	5140	90	180	84
27		466	1.37	5220	90	184	85
28		480	.74	3390	66	121	58
29		482	.94	3790	68	142	66
30		487	1.92	4890	--	185	--
31		489	1.85	4910	--	182	--
32		492	1.50	5080	89	186	86
33		493	1.58	5130	91	189	88
34		499	1.37	5010	86	176	81
35	3	414	1.45	5230	91	178	82
36	(see fig.	415	1.39	5190	90	184	85
37	1(c))	416	1.15	5050	88	173	79
38		417	.95	4760	86	164	76
39		418	1.48	5270	92	181	84

[a]Theoretical values based on equilibrium composition; chamber pressure, P_c, 600 lb/sq in. abs (figs. 13 and 14).

[b]Experimental specific impulse for convergent nozzle expanded to ambient conditions.

[redacted]

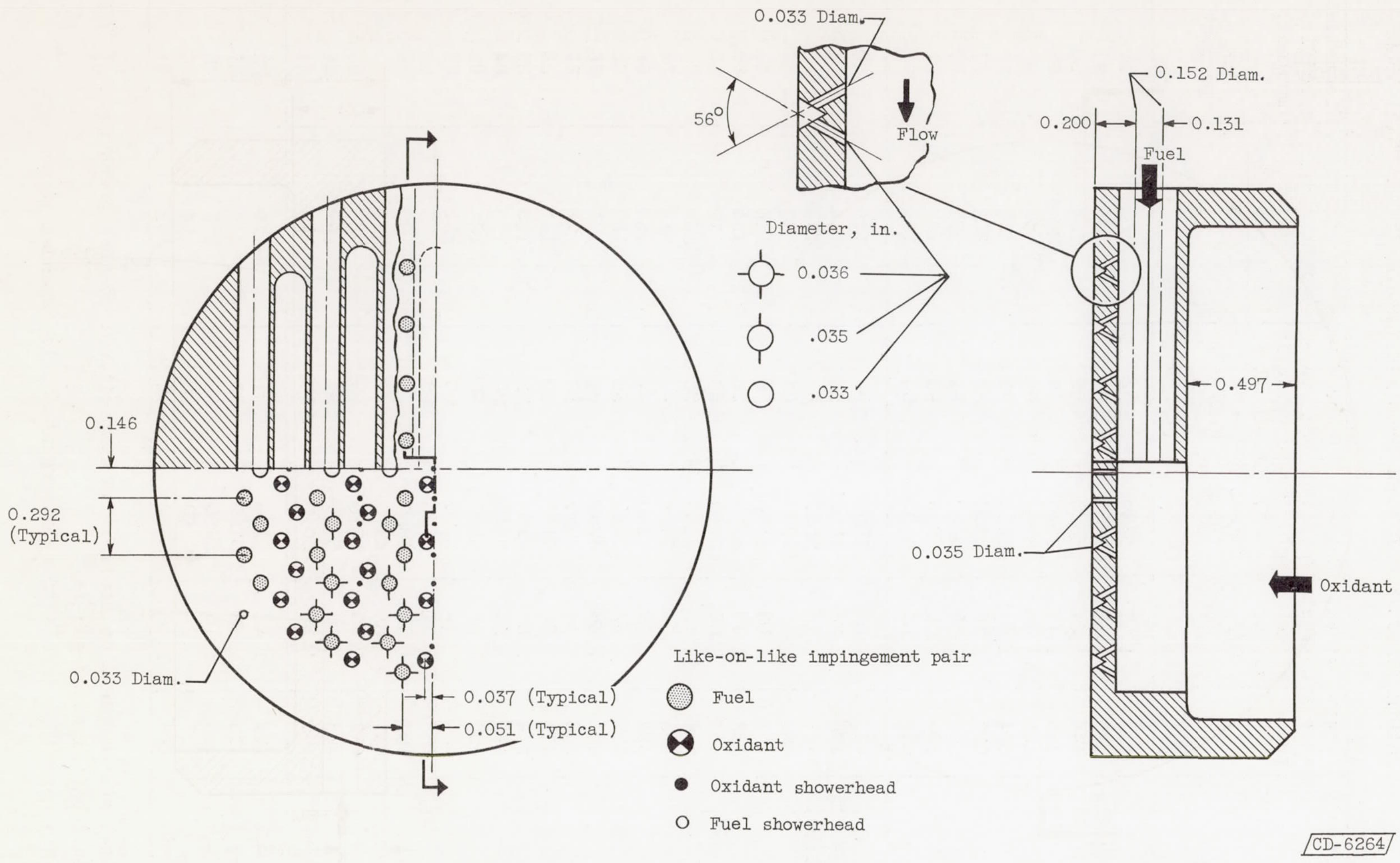

(a) Injector 1; 70 pairs of like-on-like fuel holes, 66 pairs of like-on-like oxidant holes with surface impingement at 56°; 27 showerhead oxidant holes, 4 showerhead fuel holes.

Figure 1. - Injector design. (All dimensions in inches.)

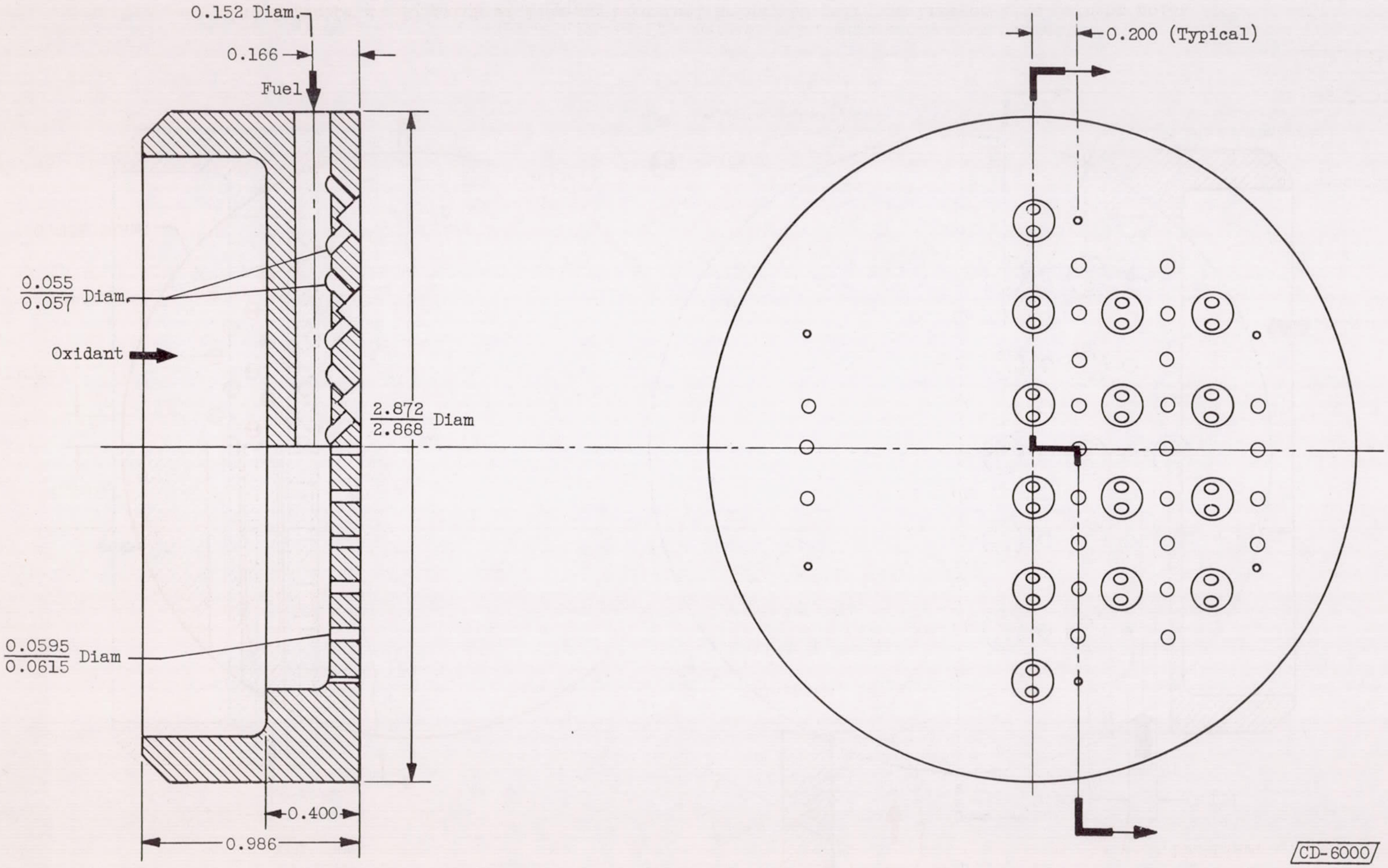

(b) Injector 2; 22 pairs of like-on-like fuel holes with surface impingement at 90°; 22 showerhead oxidant holes.

Figure 1. - Continued. Injector design. (All dimensions in inches.)

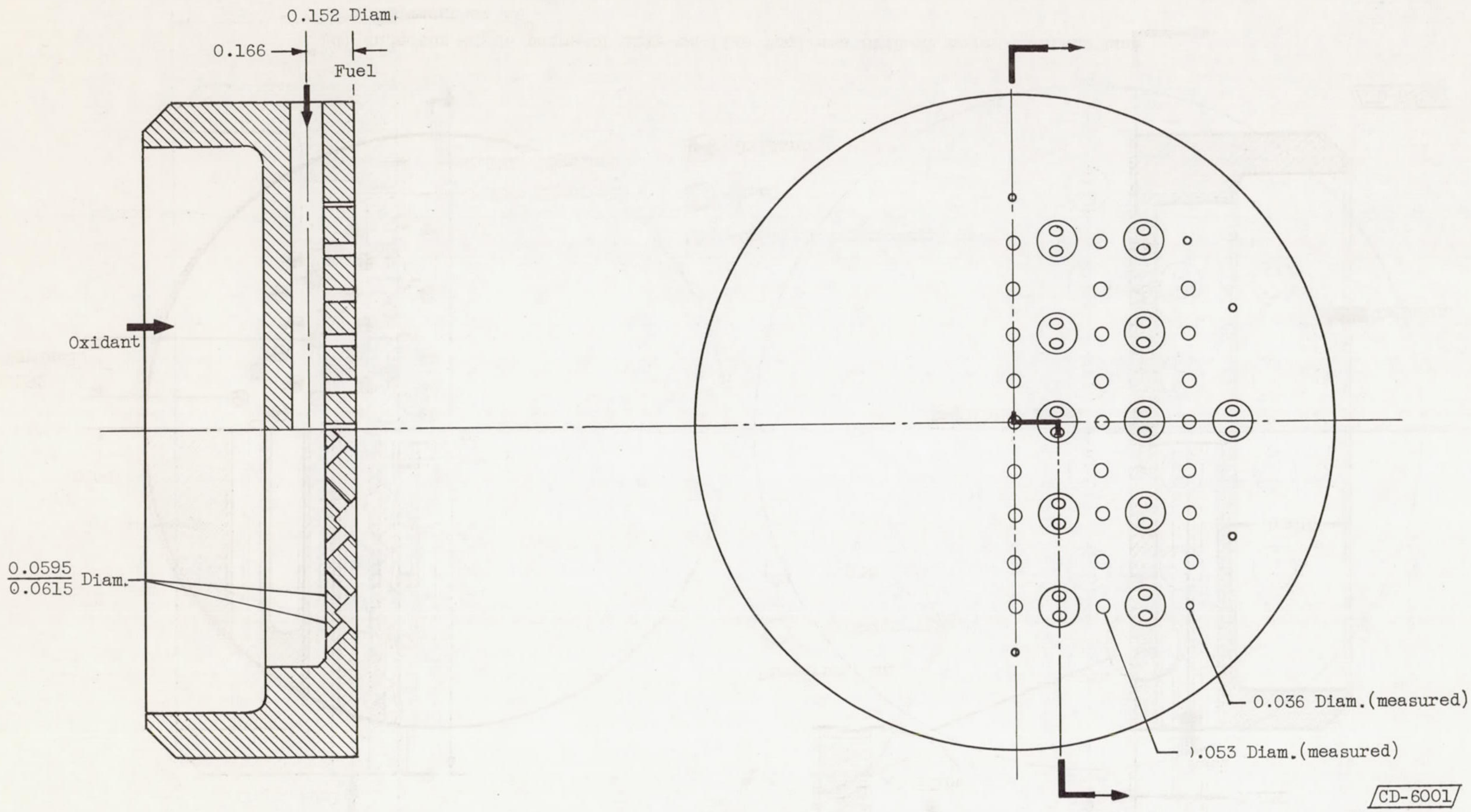

(c) Injector 3; 22 pairs of like-on-like oxidant holes with surface impingement at 90°; 22 showerhead fuel holes.

Figure 1. - Continued. Injector design. (All dimensions in inches.)

[redacted]

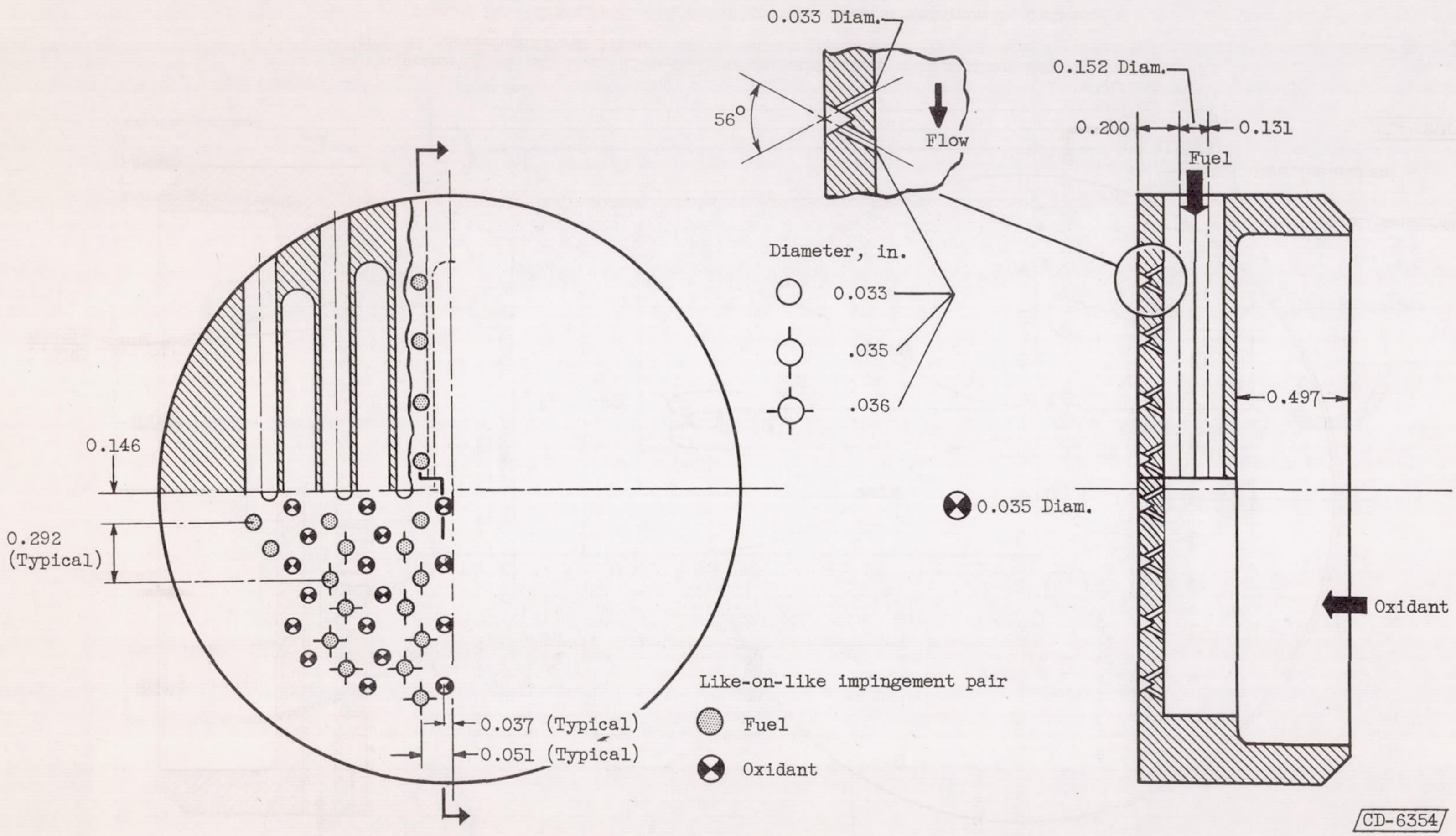

(d) Injector 4; 66 pairs of like-on-like fuel and oxidant holes with surface impingement at 56°.

Figure 1. - Concluded. Injector design. (All dimensions in inches.)

[redacted]

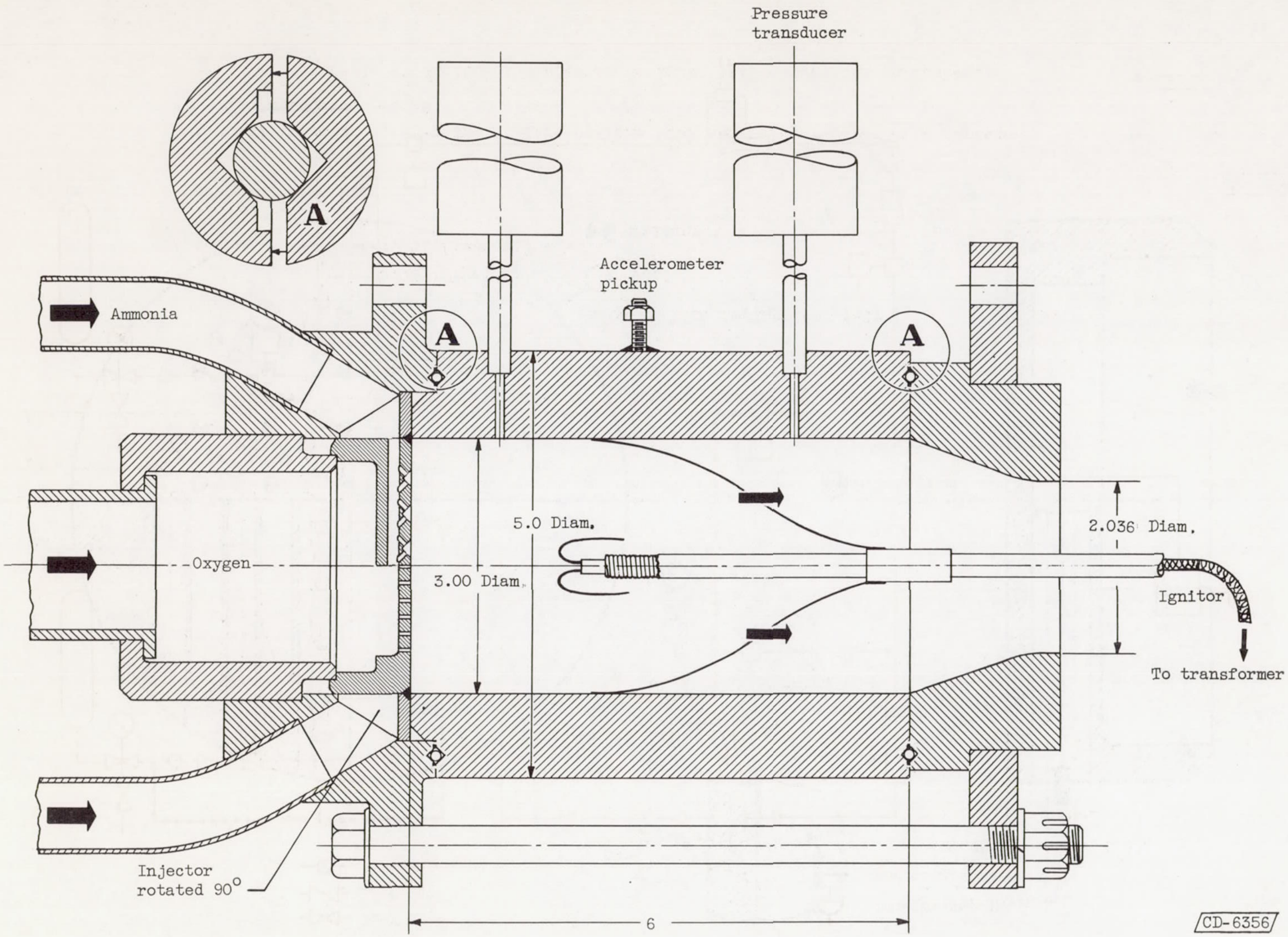

Figure 2. - Engine assembly. (All dimensions in inches.)

[redacted]

[redacted]

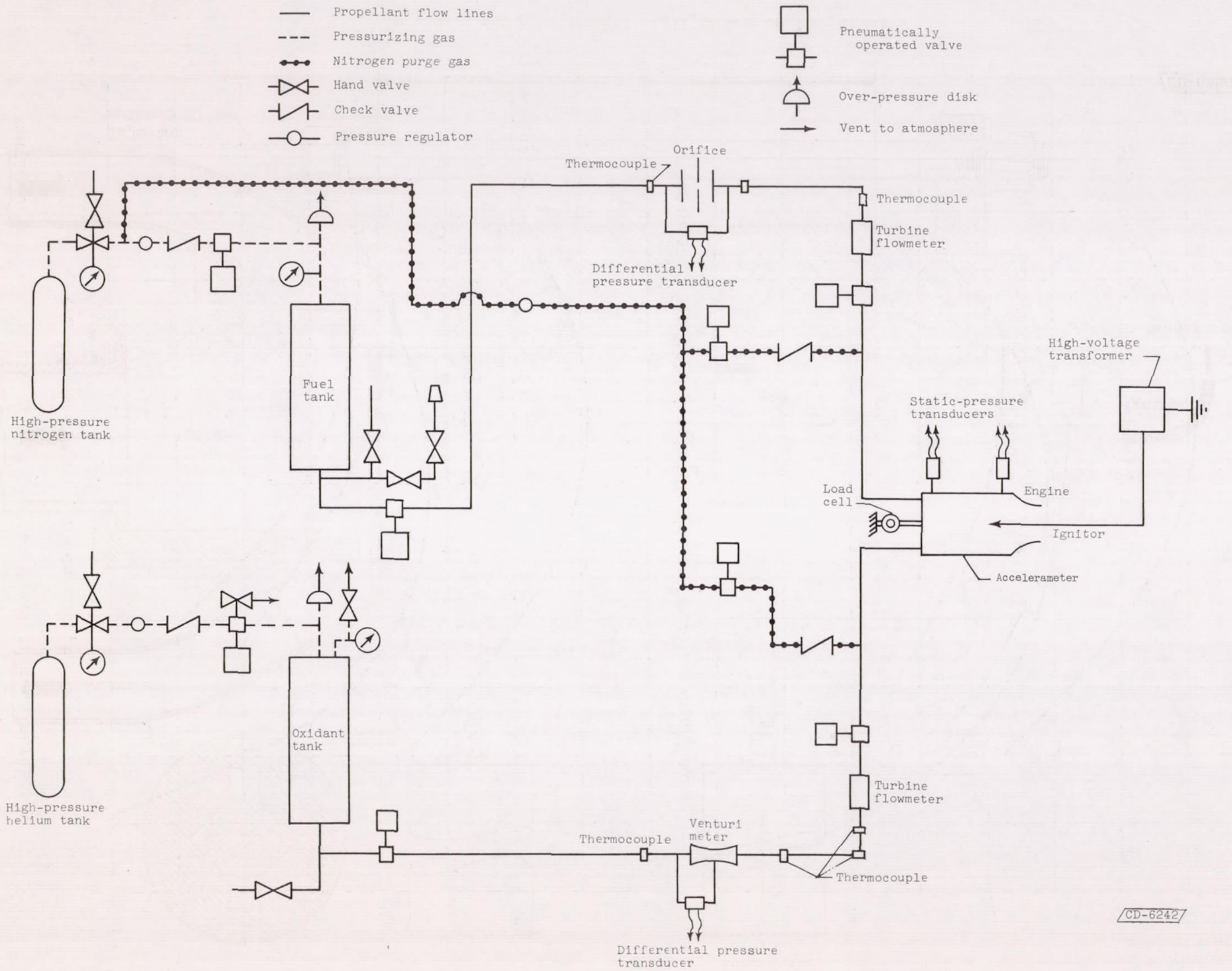

Figure 3. - Schematic diagram of test facility.

UNCLASSIFIED

[redacted]

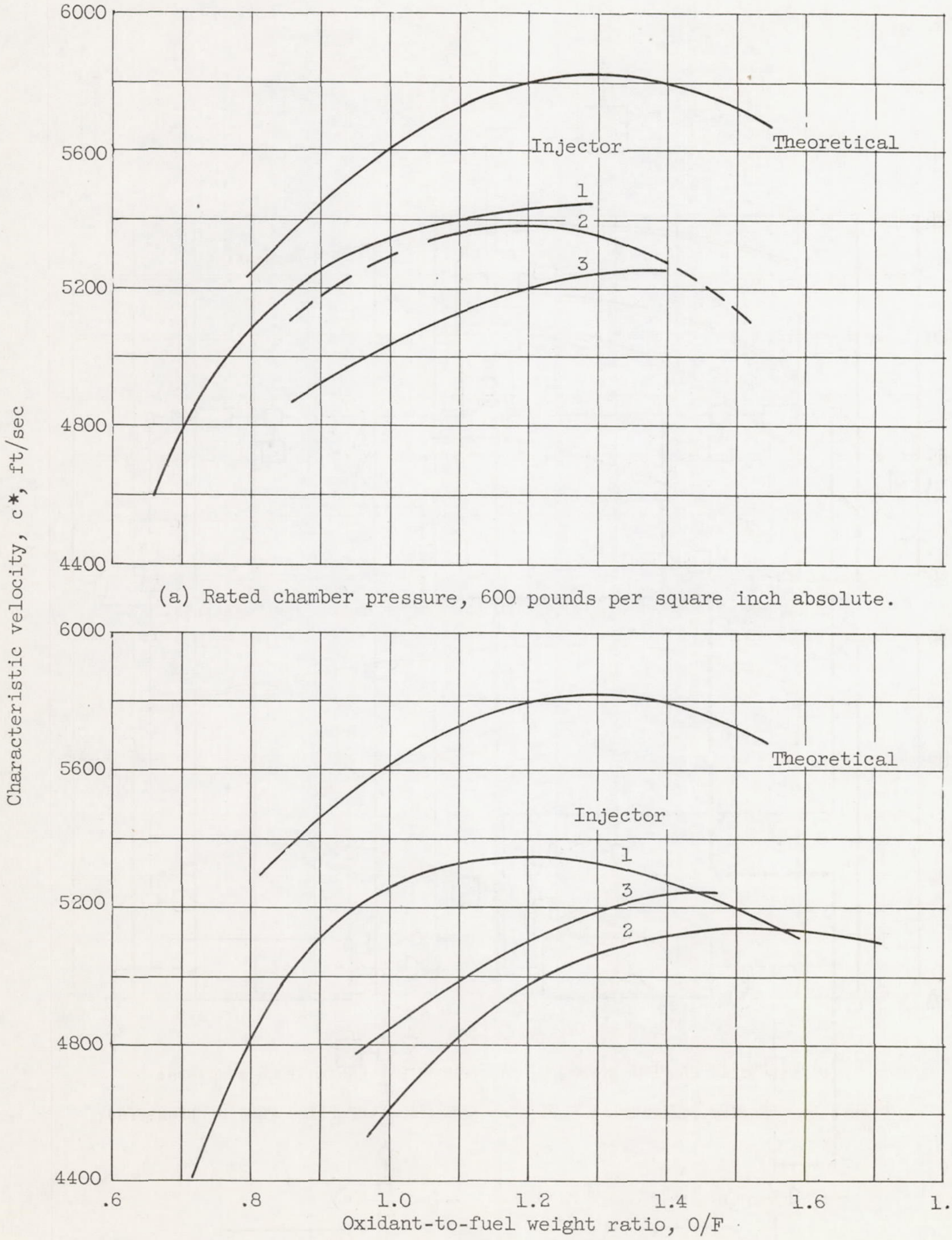

(a) Rated chamber pressure, 600 pounds per square inch absolute.

(b) Throttled chamber pressure, 360 pounds per square inch absolute.

Figure 4. - Injector performance curves at rated and throttled chamber pressures.

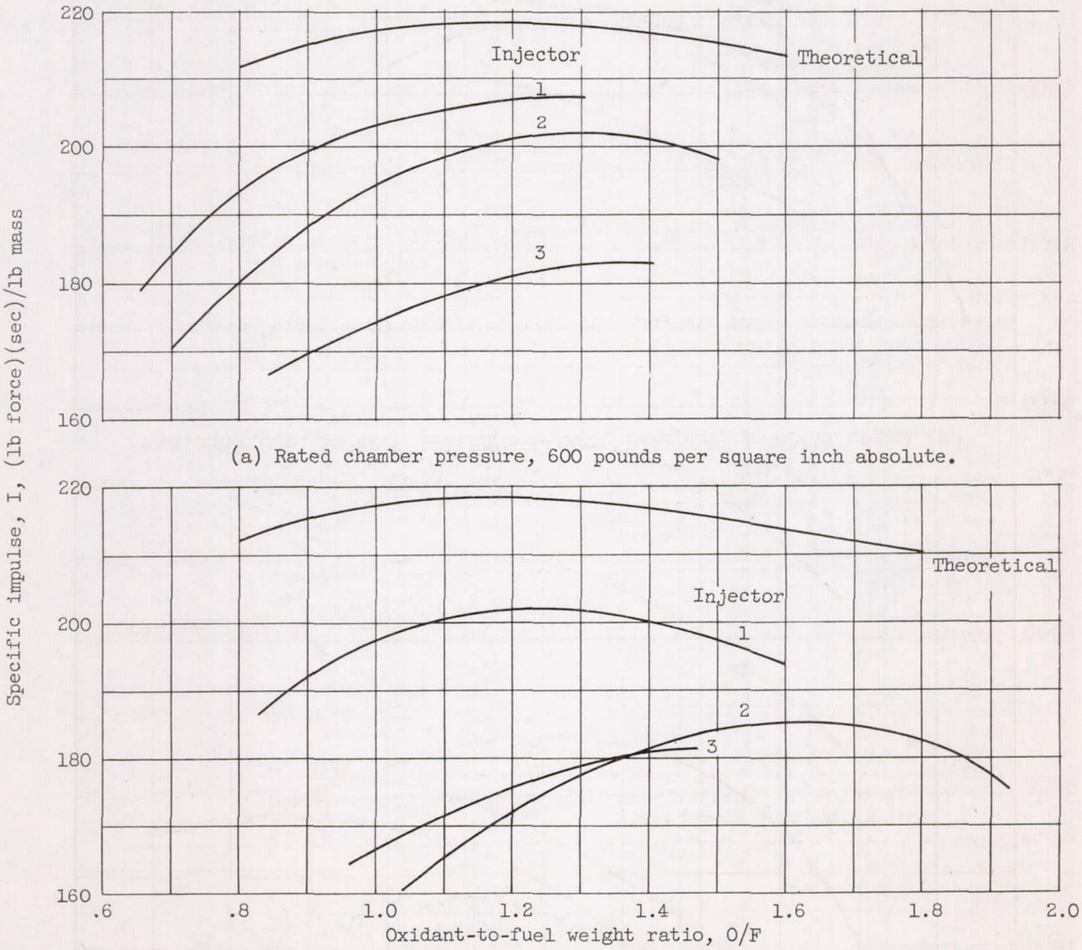

(a) Rated chamber pressure, 600 pounds per square inch absolute.

(b) Throttled chamber pressure, 360 pounds per square inch absolute.

Figure 5. - Engine performance curves at rated and throttled chamber pressures.

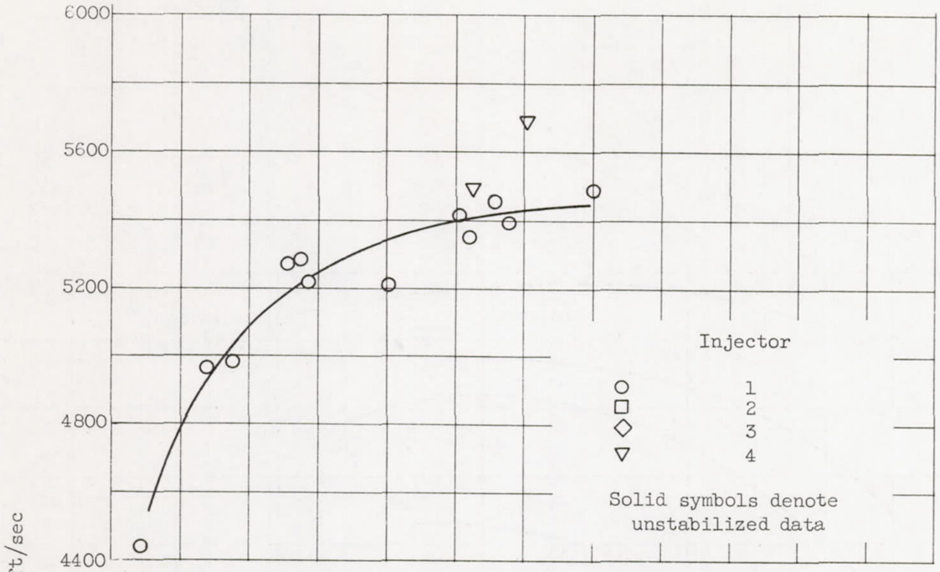

(a) Injectors 1 and 4. Fuel and oxidant like-on-like impingement, fine atomization.

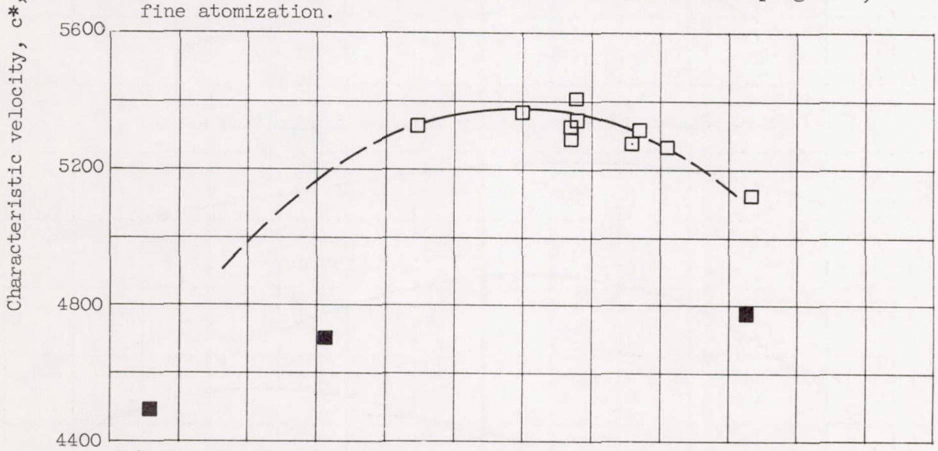

(b) Injector 2. Fuel like-on-like impingement, coarse atomization; oxidant showerhead.

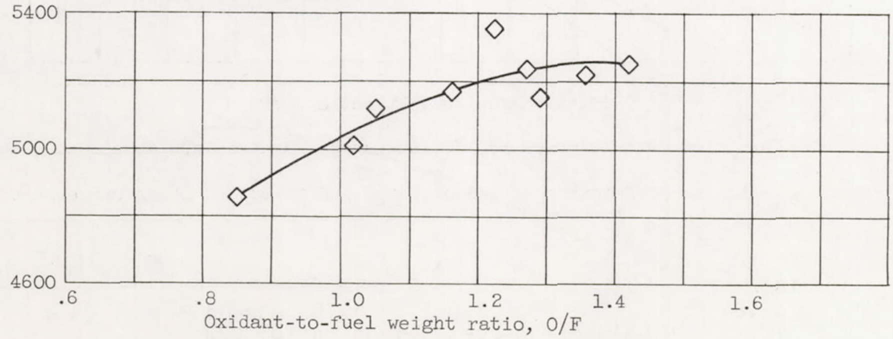

(c) Injector 3. Oxidant like-on-like impingement; fuel showerhead.

Figure 6. - Injector performance at nominal chamber pressure of 600 pounds per square inch absolute.

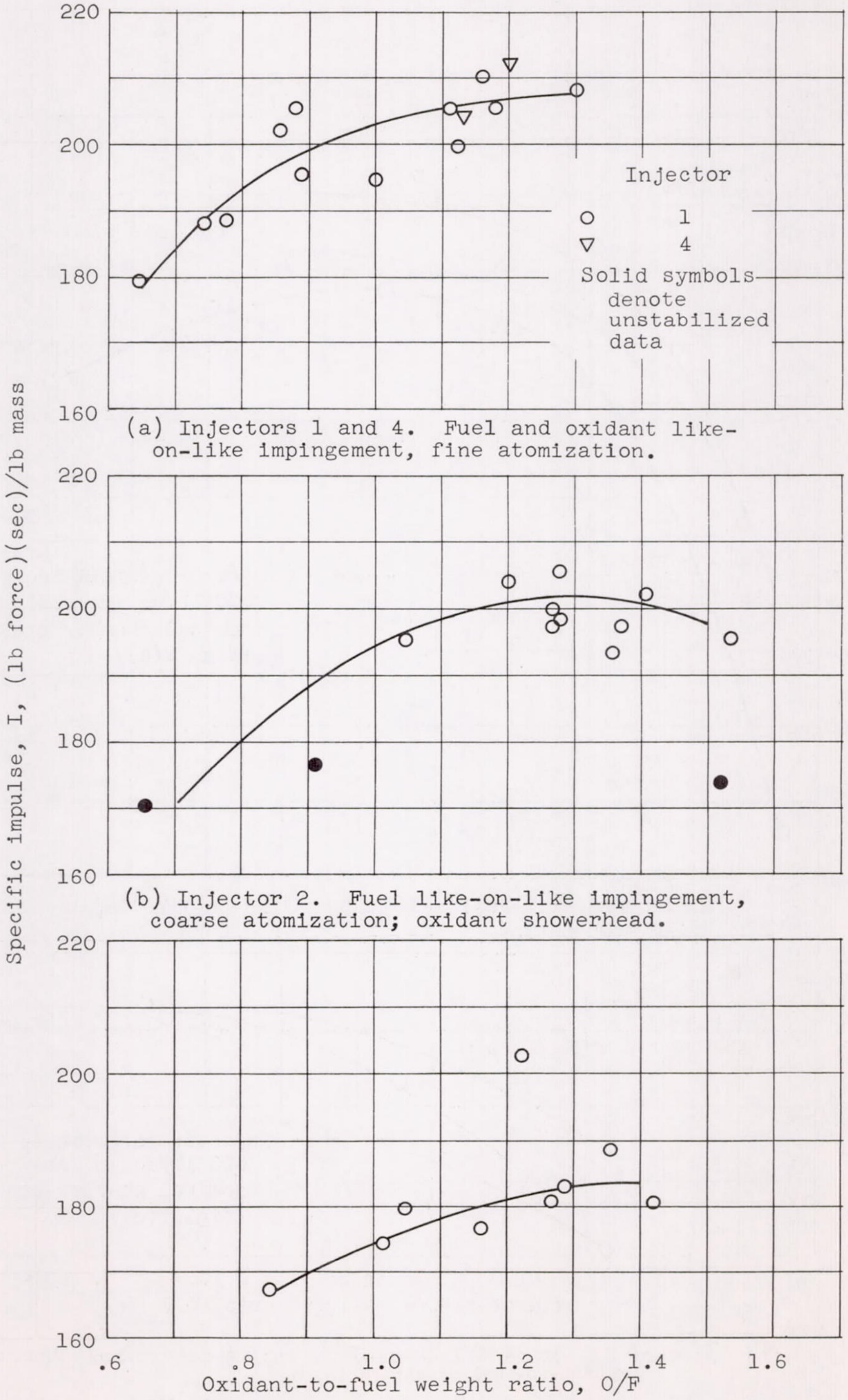

(a) Injectors 1 and 4. Fuel and oxidant like-on-like impingement, fine atomization.

(b) Injector 2. Fuel like-on-like impingement, coarse atomization; oxidant showerhead.

(c) Injector 3. Oxidant like-on-like impingement; fuel showerhead.

Figure 7. - Engine performance at nominal chamber pressure of 600 pounds per square inch absolute.

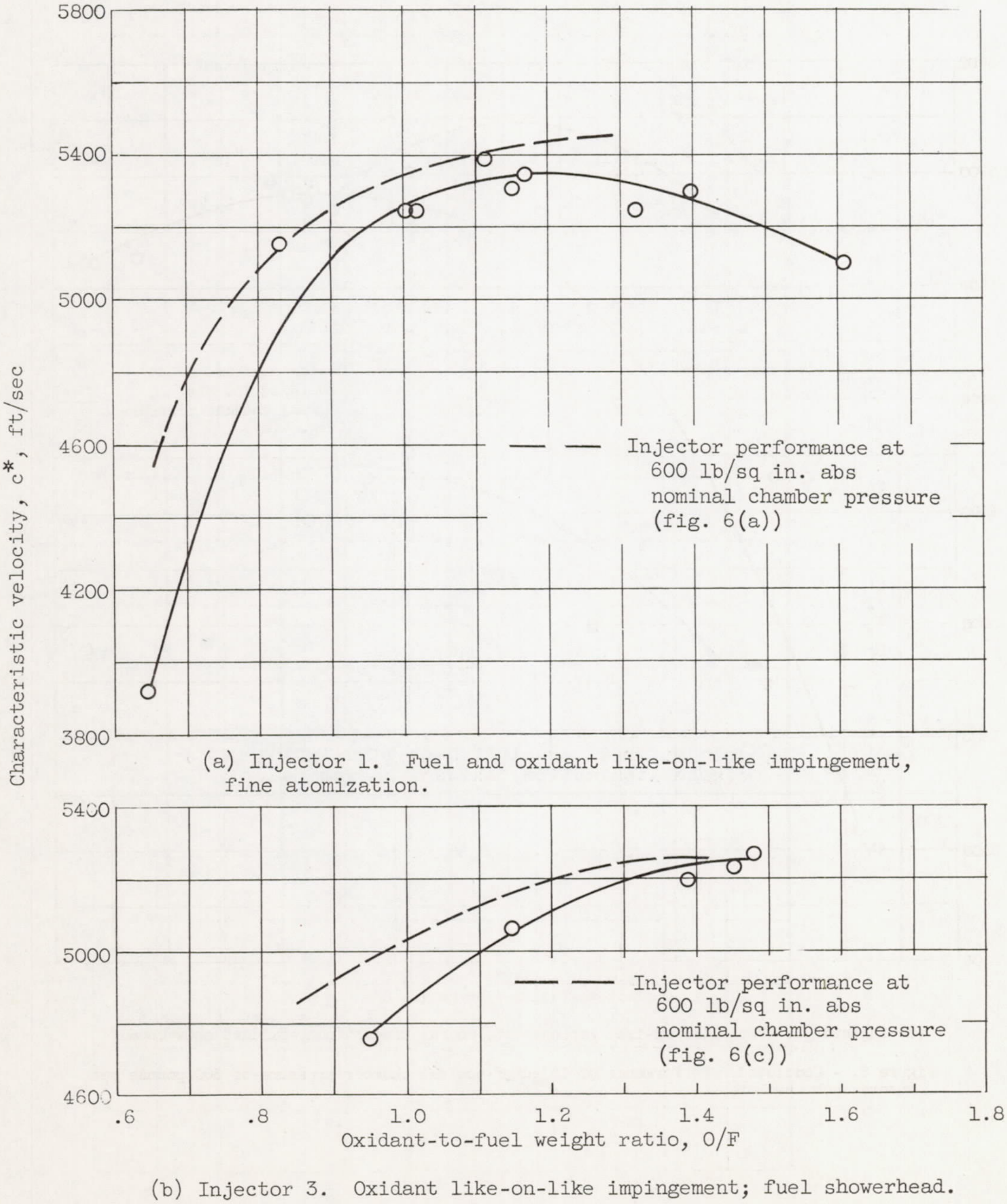

(a) Injector 1. Fuel and oxidant like-on-like impingement, fine atomization.

(b) Injector 3. Oxidant like-on-like impingement; fuel showerhead.

Figure 8. - Performance of injector at nominal chamber pressure of 360 pounds per square inch absolute.

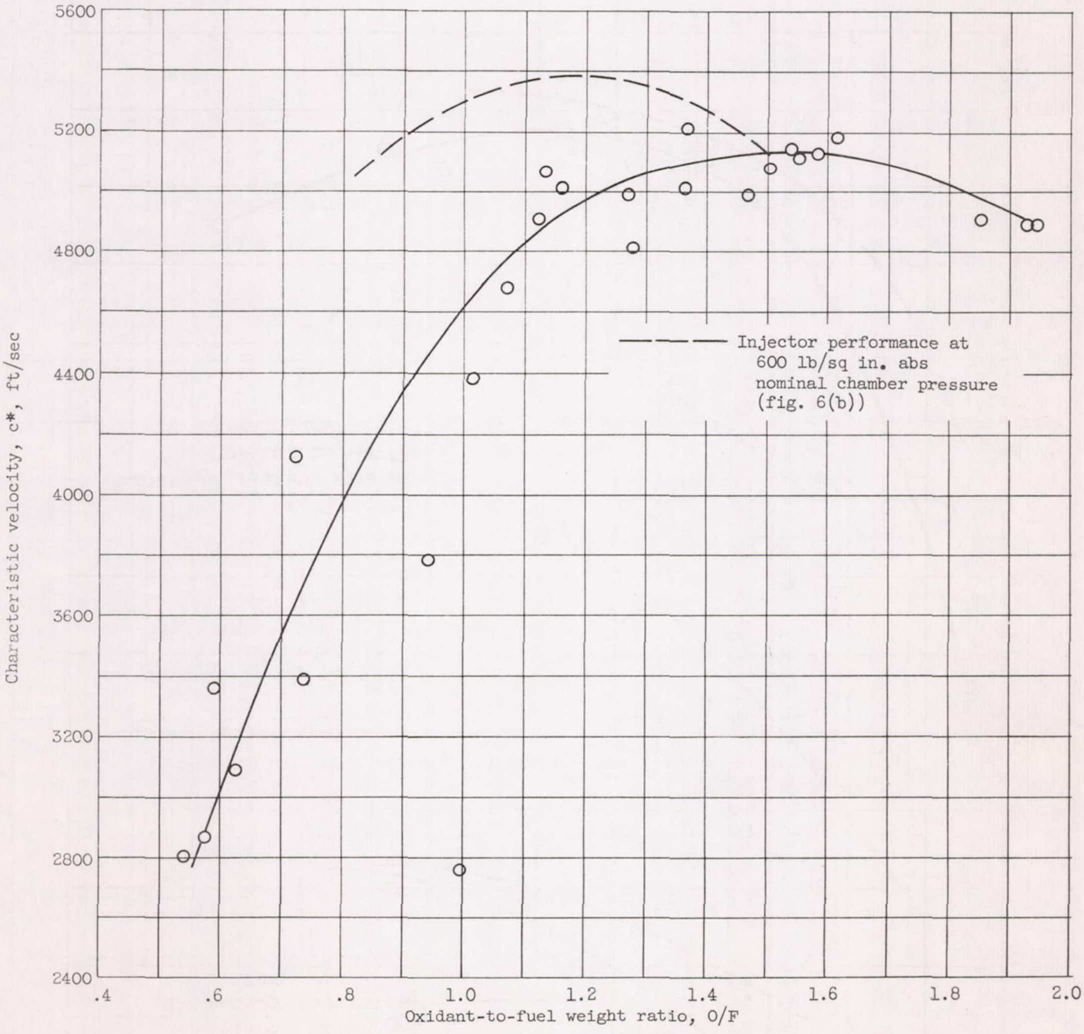

(c) Injector 2. Fuel like-on-like impingement, coarse atomization, oxidant showerhead.

Figure 8. - Concluded. Performance of injector nominal chamber pressure of 360 pounds per square inch absolute.

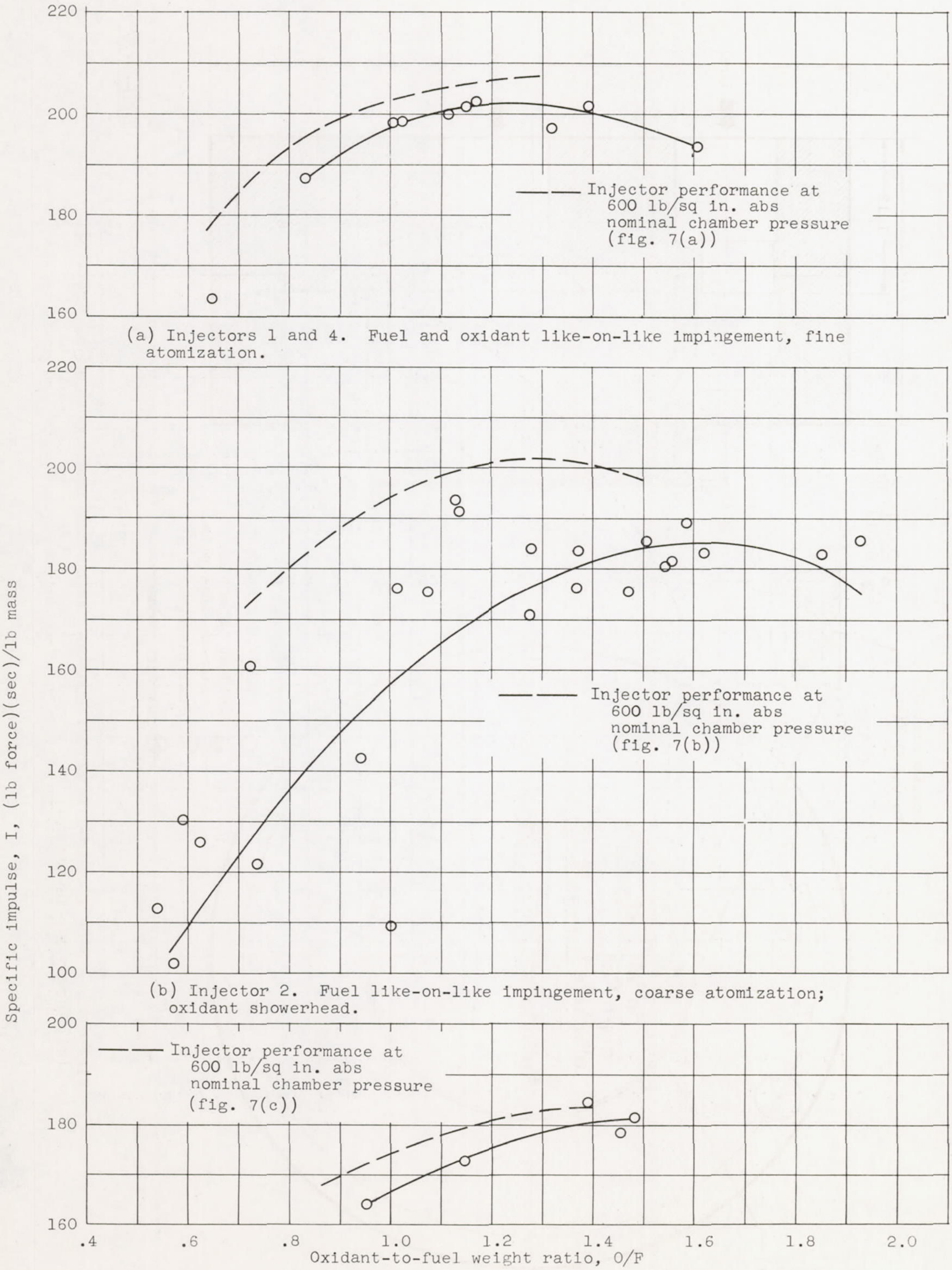

(a) Injectors 1 and 4. Fuel and oxidant like-on-like impingement, fine atomization.

(b) Injector 2. Fuel like-on-like impingement, coarse atomization; oxidant showerhead.

(c) Injector 3. Oxidant like-on-like impingement; fuel showerhead.

Figure 9. - Engine performance nominal chamber pressure of 360 pounds per square inch absolute.

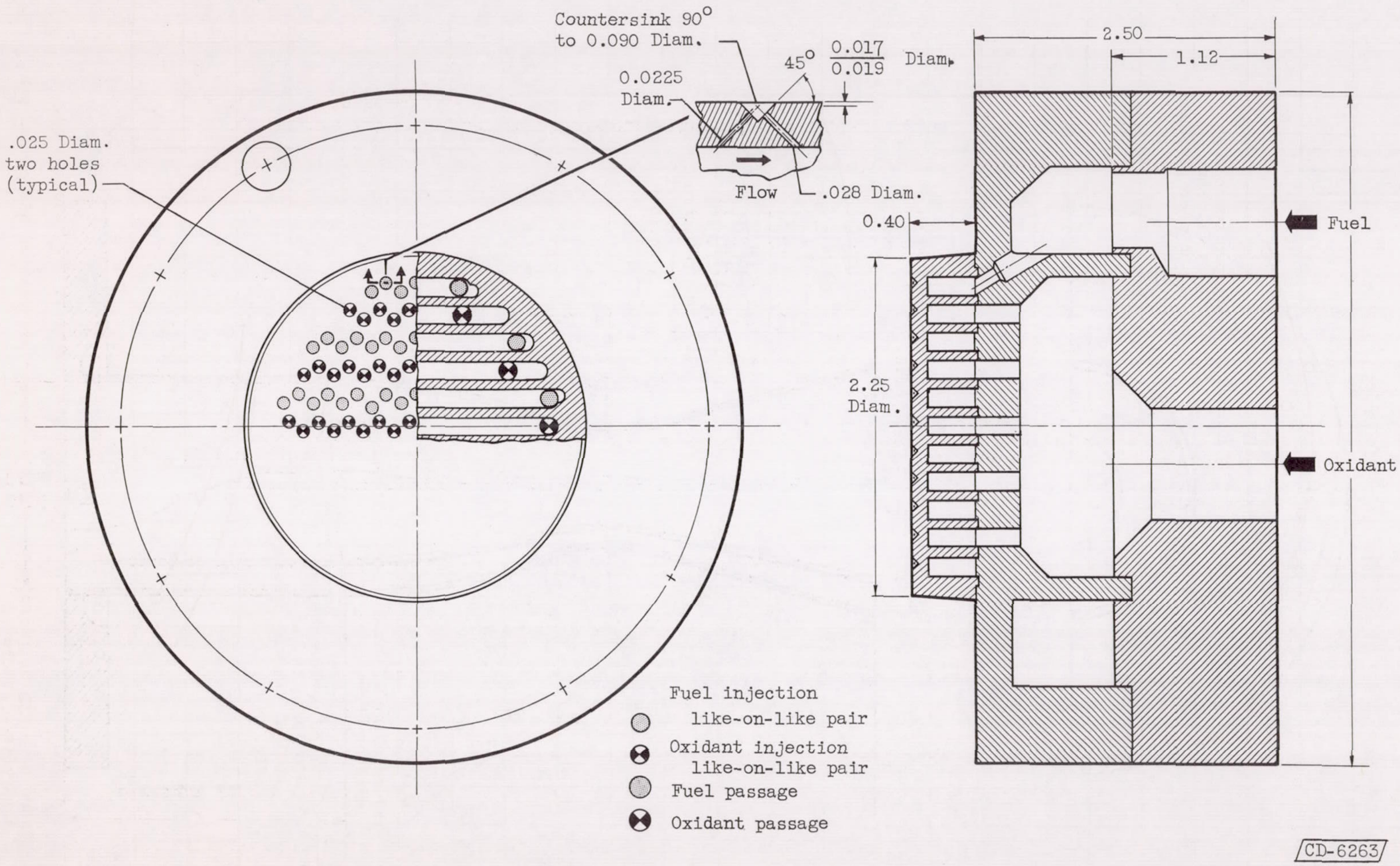

Figure 10. - NACA 1K-4-AO-1 injector; like-on-like surface impingement at 90° (ref. 2). (All dimensions in inches.)

[redacted]

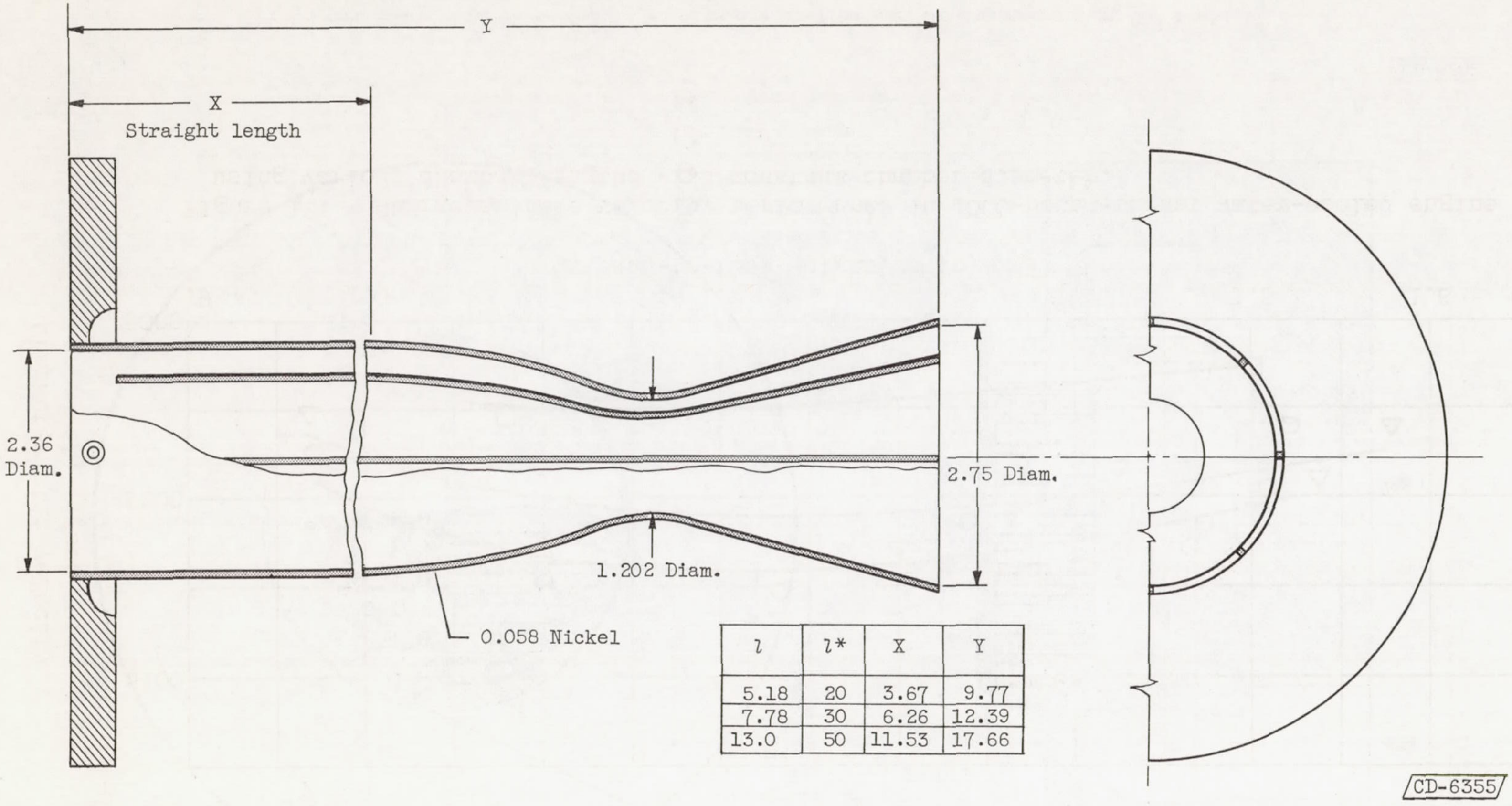

l	l^*	X	Y
5.18	20	3.67	9.77
7.78	30	6.26	12.39
13.0	50	11.53	17.66

Figure 11. - Chamber for 1000-pound-thrust water-cooled engine. (All dimensions in inches.)

[redacted]

[redacted]

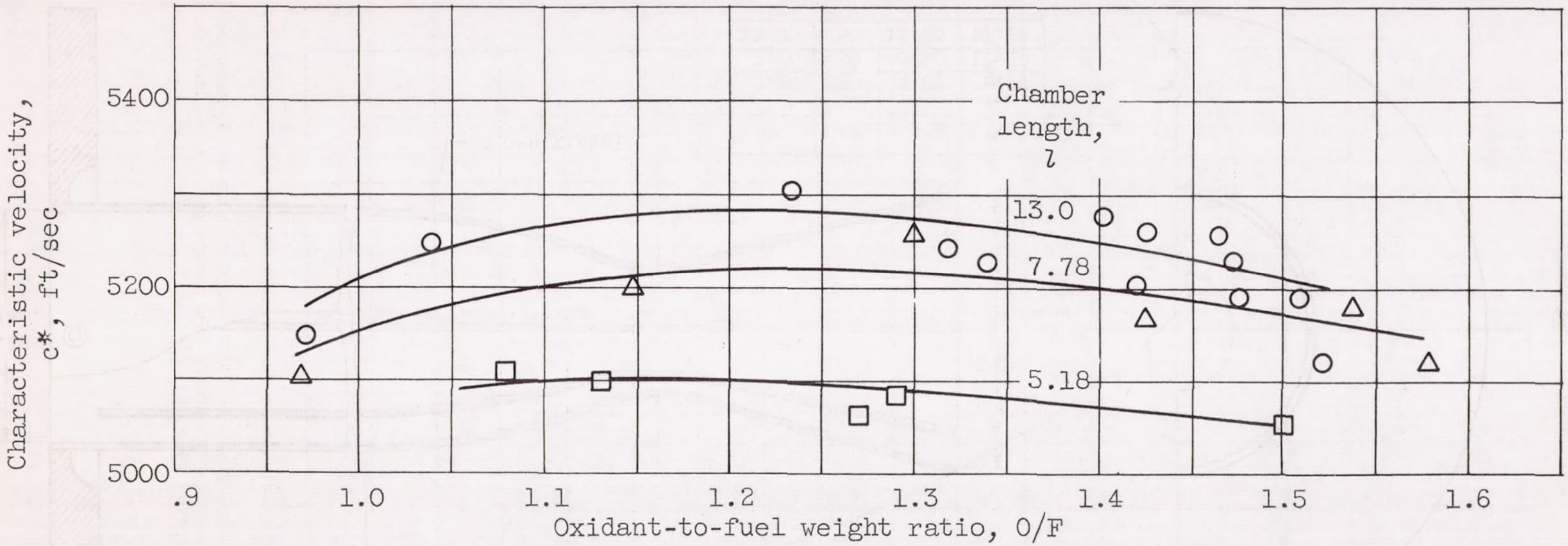

Figure 12. - Characteristic velocity performance in 1000-pound-thrust water-cooled engine using various chamber lengths with constant chamber diameter.

[redacted]

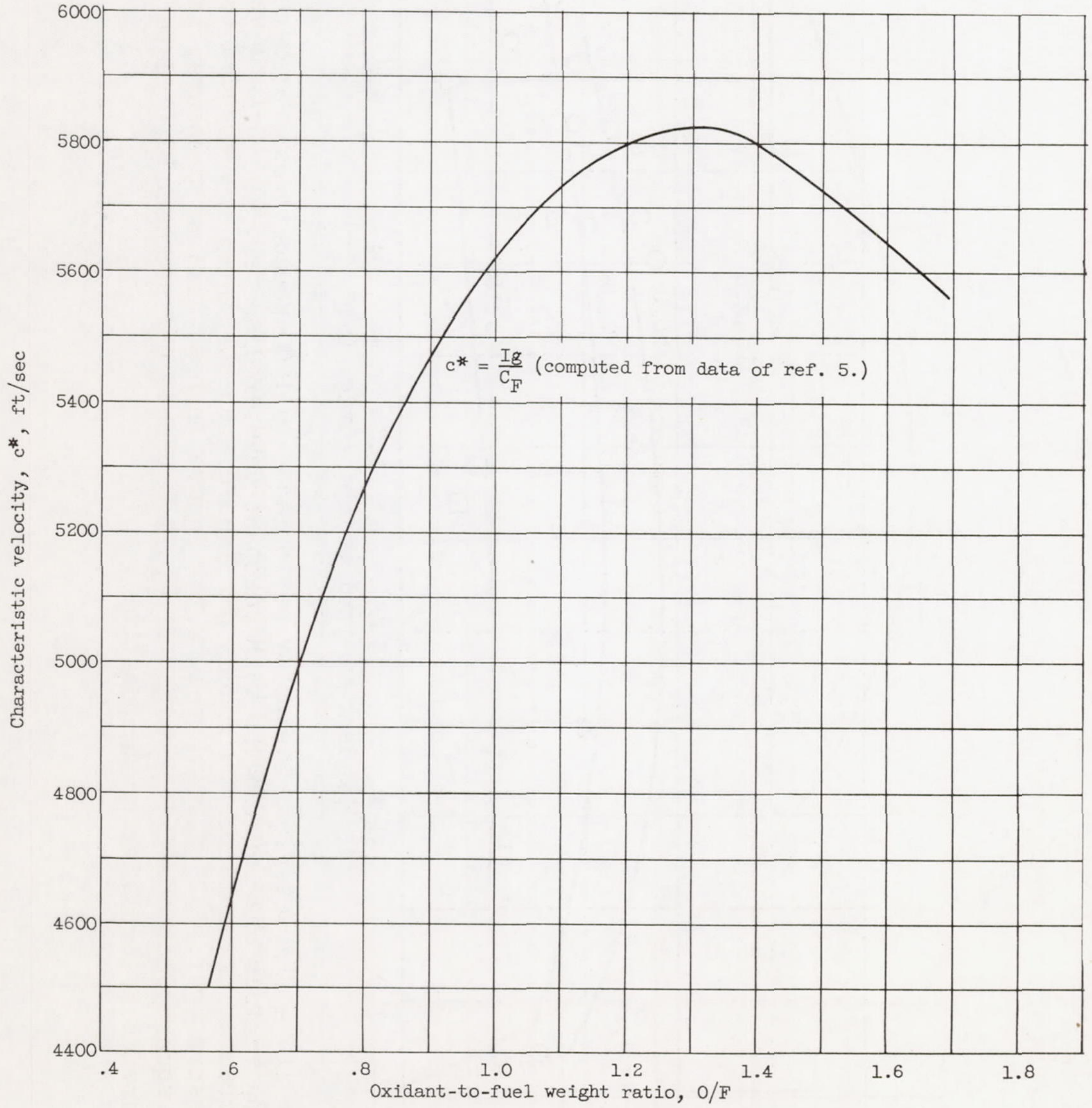

Figure 13. - Theoretical characteristic velocity plotted against oxidant-to-fuel weight ratio at chamber pressure of 600 pounds per square inch absolute. Equilibrium composition (ref. 6).

[redacted]

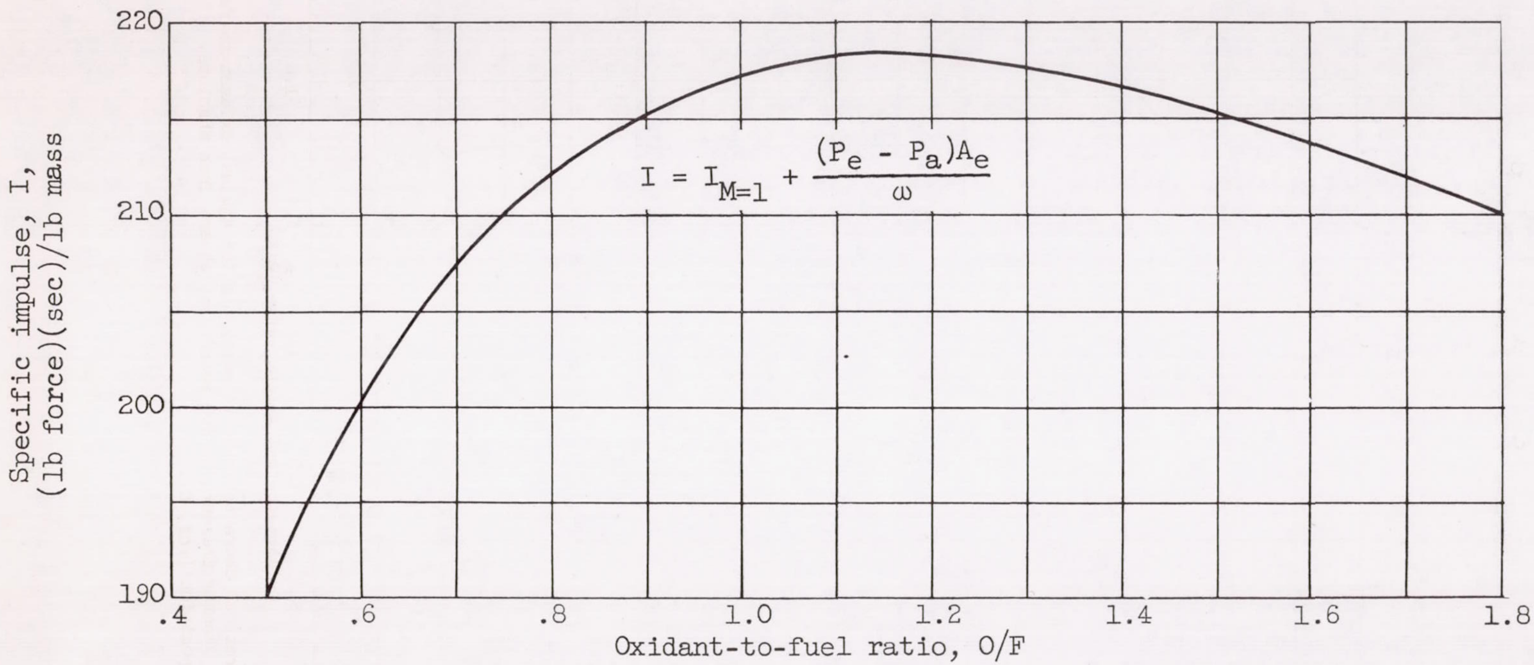

Figure 14. - Theoretical specific impulse plotted against oxidant-to-fuel weight ratio at chamber pressure of 600 pounds per square inch absolute; nonexpanded to ambient pressure (ref. 6). Throat area, 2.259 square inches; ambient pressure, 14.7 pounds per square inch absolute; weight flow, 11.0 pounds per second; $I_{M=1}$ data are from reference 6 (equilibrium composition).

UNCLASSIFIED

UNCL[redacted]IED

[redacted]